

Optimization of Bumper System for Regulatory Performance and Cost Minimization

Matt Schmidt Stephanie Singer
University of Michigan | ME555 | Winter 2015

Introduction

In order to lessen the serious injuries and fatalities of vehicle-pedestrian crashes, automakers have recently increased focus on optimizing vehicle front ends for pedestrian protection. Although the US currently does not have legal regulatory requirements for pedestrian safety, most manufacturers are building vehicles for a global economy, and it is therefore necessary to consider a pedestrian's safety when designing any passenger vehicle.

Most pedestrian safety evaluations test the impact of a leg form dummy on the vehicle's front fascia, a hip impactor for the bonnet/upper fascia, and a head form dummy is used on the hood. While these three areas are in close proximity on the vehicle, the design criteria governing the hood and bumper are quite dissimilar, so the problem is frequently separated into many smaller optimizations. Optimization of the front bumper alone, therefore, yields an appropriate amount of complexity for this project. We will therefore consider impacts made only between the leg form and bumper when investigating pedestrian protection.

In order to further investigate front bumper fascia, the low speed collision test as dictated by ECE-R42 frontal load case, also imposes constraints. Crashworthiness is therefore a separate optimization sub-problem. The front bumper must be substantial enough to limit the cost of damage in fender-bender type accidents. The cost is interpreted as the maximum intrusion of the rigid impactor. The low speed test implements a rigid impactor at a height near the middle energy absorber of the bumper. The impactor is similar to the leg form in that it is sensor filled and may also damage other features of the car, but only the front bumper is considered in this optimization.

Although cost and styling are usually the most important design criteria for the bumper system, minimizing system cost will be the final constraint. This is sensible because pedestrian safety is unlikely to be a value-adding attribute to a car buyer: the regulations must simply be met. Similarly, the bumper must be able to withstand crash dynamics. Crashworthiness is an important, value adding metric since consumers are concerned with cost and the repercussions of low speed accidents. Our objective is therefore to minimize cost and intrusion while maximizing pedestrian protection subject to the constraints imposed by safety regulations.

Subsystem Background

Regulatory Overview

As far as vehicle regulations are concerned, the primary functions of the bumper are to minimize damage in low-speed crashes with other vehicles and to ensure that pedestrians do not suffer grievous leg injuries should they be impacted. Both Europe and the US have their own interpretations of these functions, and therefore have different regulations dictating the bumper's required capabilities. In Europe, most nations subscribe to UNECE vehicle regulations; but the US has its own set of FMVSS regulations. For a global vehicle to be effectively produced, it must meet both of these regulatory standards.

In Europe, UNECE Regulation 127, whose impact requirements are summarized in Table 1, outlines the minimum pedestrian impact criteria that must be met for vehicles to be street-legal. The regulation is divided into a leg impact test for the front bumper, and a head impact test for the hood. Since we are optimizing the front bumper and not the hood, we will discount any head impact considerations of the regulation. A sensor-filled test legform is accelerated towards the vehicle, and impacts the front bumper at 40 kph. Throughout impact, sensor data in the legform is recorded by an accelerometer and two strain rosettes. These readings are calculated into three separate criteria, each of which has a maximum threshold not to be exceeded: knee bending angle (degrees), knee shearing displacement (mm), and upper tibial acceleration (g force). A visual representation of these criteria is shown in Figure 1. A consumer protection agency, the EuroNCAP (New Car Assessment Program), also rates the pedestrian safety of European vehicles, but has stricter maximum values for all three impact criteria. The EuroNCAP awards a "green" pedestrian safety rating to vehicles which excel above regulatory limits. The criteria for this high rating are shown in Figure 1. While the US does not have regulations governing pedestrian safety, Global Technical Regulation #9 (based off of UNECE R127) is expected to be adopted in North America in the coming years [1].

Area	Measurement	Value
Lower legform/Bumper	Knee Bending Angle	19°
	Knee Shearing Displacement	6 mm
	Upper Tibial Acceleration	170 g
Upper legform/bumper	Sum of impact forces	7.5 kN
	Bending moment of Impactor	510 Nm
Headform	HIC of min. 1/2 Child Headform Area	HIC ≥ 1000
	HIC of min. 2/3 of Child/Adult Area	HIC ≥ 1000
	HIC remaining areas	HIC ≥ 1700

Table 1: Overview of UNECE 127/GTR 9 impact requirements for pedestrian impacts at 40 kph

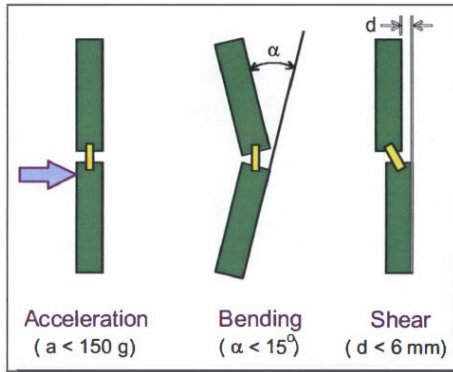


Figure 1: Representation EuroNCAP “green” pedestrian protection rating criteria for leg impact test
 Credit: Peter Schuster, *Current Trends in Bumper Design for Pedestrian Impact*

In addition to satisfying pedestrian protection regulations, a vehicle’s bumper system must also be robust in low speed vehicle-vehicle crashes. This is governed by UNECE Regulation 42 in Europe and FMVSS 581 in the US. These regulations are fairly similar, and evaluate the vehicle’s damage after it has impacted a deformable barrier at 4 kph (2.5 mph). This regulation is not related to the vehicle occupants’ safety: the bumper system would dissipate minimal energy in the high speed crashes which affect the driver or passengers. During these ‘fender-bender’ type accidents, the headlights must remain functional, the hood must not unlatch, and the vehicle must have minimal estimated repair costs. Although North American regulators are notoriously relaxed in their accurate assessment of this test, European consumers are highly interested in bumper effectiveness for small accidents, as the insurance cost indices in Europe are heavily consulted when purchasing a vehicle. In all UNECE-regulated nations, RCAR bumper testing plays a large part in vehicle’s insurance cost index, and the IIHS evaluates bumpers similarly for consumers in the US. The specifications for these consumer protection agencies are shown below in Table 2, as well as their regulatory counterparts. After the specified impact occurs with a deformable barrier, the cost to repair the vehicle is calculated.

Bumper Test Procedures

	Frontal		Corner		
	Barrier Height (mm to bottom edge)	Velocity (Km/hr)	Height (mm)	Velocity (Km/hr)	Type
RCAR	405	10	405	5	15% offset
ECE 42	445	4	445	2.5	60° angle
FMVSS 581	409-505	4	409-505	2.4	10% offset
IIHS	457	10	406	5	15% offset

Table 2: Regulatory and consumer protection low speed impact evaluation parameters

In general, a soft bumper system is desired for pedestrian protection, but a hard bumper system is necessary to minimize damage to forward components (hood, headlights, radiator). These regulations themselves present an optimization problem, but they are only a portion of the objective of front end optimization.

Cost and Manufacturing Assumptions

The automotive industry constantly strives to reduce costs and remain competitive. Just as the front bumper design must comply with regulations, it must also be inexpensive in order to be produced by a manufacturer. Surveying some common designs allowed assumptions about what materials and dimensions were typical of a front bumper. Further investigation gave insight into common production methods and the costs involved. This research gave us the information necessary to develop a cost model to be optimized.

A typical bumper is comprised of several energy absorbers behind a plastic fascia. The fascia is a molded plastic piece which frames the grill and headlights, and is often regarded as the vehicle's anthropomorphic face. The energy absorbing components of the bumper system are attached to the rear of the fascia or the front of the car's metal frame. These energy absorbers are almost always plastic, or a plastic derived product. Almost all vehicles have a middle energy absorber, placed directly behind the leading edge of the bumper, and some vehicles have multiple energy absorbers behind the fascia. From research, it seems there are a few common materials used in these energy absorbers: Expanded Polypropylene Foam (EPP), Polypropylene (PP), Polycarbonate/Polybutylene (PC/PBT), and Acrylonitrile Butadiene Styrene (ABS). In order to explore the cost of each of these, our research considered the material cost was considered alongside the processing cost to find the total cost of each theoretical energy absorber. These costs are combined into a price per kilogram [\$ USD/kg] value, shown below in table 3.

Out of these four options, EPP is the most conventional and inexpensive. EPP is manufactured by filling a mold with foam beads, then closing the mold and exposing the contents to a steam flash, causing them to expand and assume the shape of the mold. This process is typically accomplished in a multi-mold tool, meaning that a single station can produce multiple energy absorbers at a time. The resulting energy absorber will be the softest of all evaluated material options, but is surprisingly stiff for a foam. It is worth noting EPP is almost 50 times less dense than all other options, but also that it comparatively has a very low compressive modulus (E). The material cost comprises more than 90% of the total price per kilogram value of EPP: flash steaming the beads is neither energy intensive nor time consuming [2].



Figure 2: Comparison of EPP (left) energy absorber with typical thermoplastic (right). Note that the EPP absorber is solid, while the thermoplastic uses ribs and a more skeletal structure.

The other material options (PP, PC/PBT, and ABS) are thermoplastics, and are made into energy absorbers through injection molding. This process is considerably more expensive, as the stock material must be liquefied at high temperatures, then extruded at high pressures into a mold and solidified. In order to understand the cost-adding process of injection molding, the team used a publicly available cost simulator. The “Java Injection Molding Cost Estimation Tool” was developed at the University of Massachusetts Lowell, and is a simple yet accurate tool to comprehend the factors affecting the cost to injection mold. The program separates plastics by their melting points and stiffnesses and gives a necessary injection pressure, output, and some comments. It also gives typical thicknesses/occupancy percentages for each plastic: this occupancy percentage is the portion of the total occupied volume that is occupied with molded material. For stiffer plastics, the energy absorber can have thinner skeletal sections, and therefore the percentage of material per package space decreases with increasing compressive modulus. We assume that each of these injection molded energy absorbers is manufactured using a single material injection gate, located at the front-center of the absorber. For a low-stiffness plastic like PP, only 6.5 MPA are needed to manufacture an energy absorber with typical dimensions (2000mm X 40mm X 85mm), but over 10 MPA is necessary for hard plastics like PC/PBT or ABS. Because there is no way to import/export data from the injection molding simulator, it was necessary to create a model approximating the cost of each molded absorber [3]

Larger absorbers have a process cost which is proportionally higher than smaller absorbers. This is because of the extra mold-flow considerations. In reality, injection molding is a very complex process, often having different methodology for each individual part. For simplicity, processing cost is considered to be linear with total energy absorber mass (with a different slope for each material). Combining this information with some material price data allows for an approximate \$/kg, including material and processing costs, to be calculated for each thermoplastic material [Schroeder].

Material	\$ USD/ kg	ρ [g/ cm ³]	E [GPa]	% Occupancy	\$ USD/mm ³	\$ USD/ mm ³ Occupancy [x 10 ⁻⁷]
ABS	4.50	1.04	2.5	0.20	4.68×10^{-6}	9.36
EPP	1.93	0.20	0.4	1.00	3.86×10^{-7}	3.87
PC	2.30	0.95	1.4	0.25	2.18×10^{-6}	5.44
PC/PBT	3.98	1.20	1.9	0.20	4.78×10^{-6}	9.55

Table 3: Cost calculation of energy absorbers. \$/kg values taken from [Java], [CAR]

While real-world cost considerations are far more complicated and specific than the ones described here, our assumptions lead to a reasonably accurate, if not conservative, cost model.

Model Construction

Variable Selection

There are many ways to model the bumper system when considering pedestrian safety and low-speed damageability or crashworthiness. Most models consider three load paths: a top, middle, and bottom, as shown in Figure 3 below. Each load path represents an energy absorber (or another concentration of stiffness) hidden behind the front bumper, usually made out of foam or plastic. The heights of each load path off the ground are important design variables for pedestrian safety, as they must have some relation to the anatomical test legform (3 variables). The middle energy absorber should always be the forward-most component, so the inboard offset of upper and lower absorbers is described as the distance from the front of the middle energy absorber (2 variables).

In a real-world design scenario, the middle load path is the only one guaranteed to have a dedicated energy absorption element. The upper load path many times gets its stiffness from innovative fascia/bonnet shapes which allow for cost and space savings. The lower load path is typically comprised of a very thin sheet of plastic, a metal bar, or another cost-saving solution. The energy dissipation strategies of the upper and middle load paths will likely be determined by other design objectives for the vehicle, so instead of specifying the shape and material of the upper and lower load paths, we consider them for their observed stiffnesses from an outboard location (2 variables).

The middle load path, however, is an area specifically dedicated to the bumper. For the middle load path, a discrete variable represents the compressive modulus of the material chosen for the absorber. This variable (E_m) can take 4 values corresponding to EPP, PP, PC/PBT, or ABS material. The height and inboard depth of this absorber are also considered as design variables in order to calculate both cost and observed stiffness of the middle load path from an outboard location.

To summarize, the model uses 10 variables, shown below in Figure 3 and Table 4. All of these variables are continuous except for the compressive modulus of the middle energy absorber, which is parameterized given based on the material selection of this load path. This set of variables gives a good approximation of the bumper system while maintaining reasonable complexity.

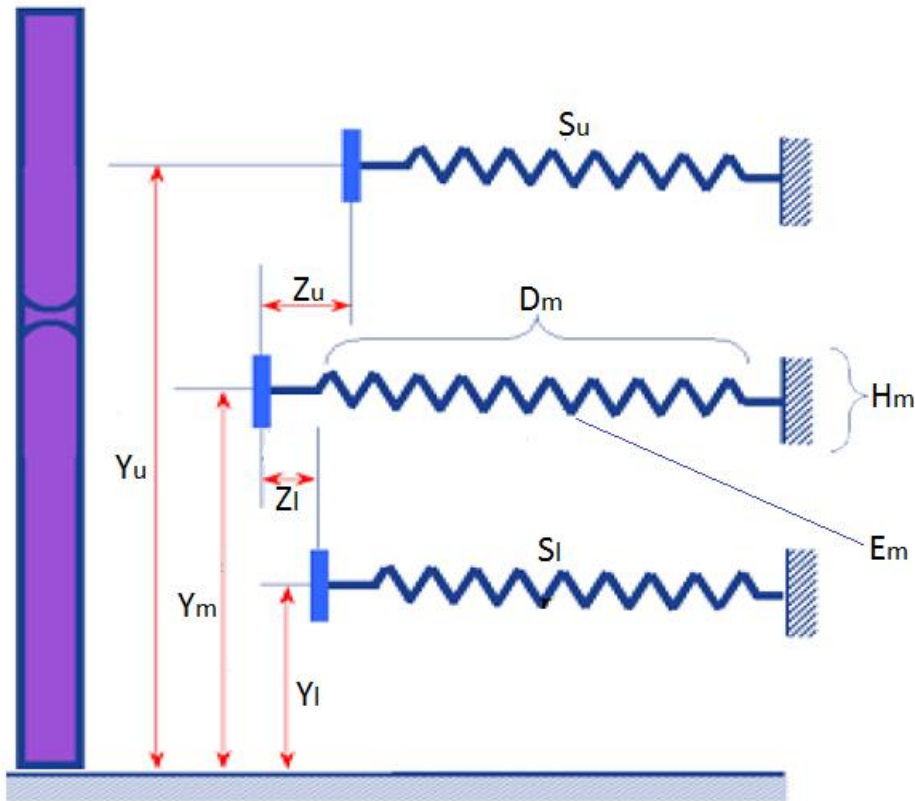


Figure 3: a visual representation of the problem with our design variables. The left structure is the pedestrian legform

Variable	Abbreviation	Variable Description
x(1)	Dm	In-board Depth of Middle Energy Absorber
x(2)	Zu	Longitudinal offset of Upper Energy Absorber
x(3)	Zl	Longitudinal offset of Lower Energy Absorber
x(4)	Hm	Height of Middle Energy Absorber
x(5)	Ym	Vertical Position of Middle Energy absorber
x(6)	Yu	Vertical Position of Upper Energy Absorber
x(7)	Yl	Vertical Position of Lower Energy Absorber
x(8)	Em	Compressive modulus of chosen material
x(9)	Su	Stiffness of Upper Energy Absorber
x(10)	Sl	Stiffness of Lower Energy Absorber

Table 4: Variable names and descriptions

Model Constraints

Given the pedestrian protection and crashworthiness equations, the following constraints are applied to the optimization problem at hand:

$$x \geq 0$$

Such that all variables or dimensions are positive numbers.

$$Y_l \geq H_{min}$$

$$Y_u \leq H_{max}$$

$$H_m \leq Y_m - Y_l$$

$$H_m \leq Y_u - Y_m$$

$$Y_l \leq Y_m \leq Y_u$$

The above constraints ensure that the bumper has salient geometry, and that energy absorbers do not occupy the same space as one another. The lower edge of the bumper must have a ground clearance of at least H_{min} , which is set at 30mm. H_{max} , the maximum height of the hood's leading edge, is set at 650 mm, the (very high) height of a Chrysler 300 bumper.

$$50 \leq D_m \leq 120$$

D_m is depth (mm) of the packaging space. For our current simulation, D_m is limited to the above range, which is suggested from benchmarking current energy absorbers.

$$5 \leq H_m \leq 50$$

The height (mm) of each absorber from its centerline (giving the EA a total height of $2 * H_m$) is limited as not to be too large.

$$Z_u \leq 250$$

$$Z_l \leq 150$$

Z_u defines the longitudinal distance from the bumper's leading edge to the top load path of the bumper. This is given a maximum value such that the car cannot have an infinitely long bumper, and so the bonnet/hood have a reasonable shape. Similarly, Z_l , the distance from the leading edge to the lower load path, is also given a maximal value based on typical designs.

Note that all constraints limiting the design variables to maximal/minimal values are value judgements determined from research. These values are generous, and allow for a wider range of designs than is observed in typical values.

Objective Construction

To create our objective to be optimized, we include the regulatory performance and cost as separate subsystems. The regulatory performance subsystem is dependent on the vehicle's pedestrian safety and low speed vehicle-vehicle damage protection potential. The cost subsystem includes the material and processing costs of the middle energy absorber: the bumper's signature component. Based on the

organizational needs of the manufacturer, these subsystems can be given different weights based on design aspirations. This is shown below in Equation 1, our objective function to be minimized.

$$\text{Min } f(x) = w * \text{Performance} + (1 - w) * \text{Cost} \quad \text{Eq. 1}$$

Where w is the subjective weight of regulatory performance, ranging from 0 to 1. The regulatory subsystem is comprised of normalized values representing pedestrian safety and bumper damageability metrics.

To gauge the effective pedestrian safety of a specific design, the team surveyed literature from SAE and ASME journals. Pedestrian impact is a difficult problem to model, but because the variables and parameters represent a standardized approach to the problem, there is a wealth of research that can be used. A study was identified which relates bumper design variables to performance in GTR 9 pedestrian legform testing. This study uses FEA simulation and Latin hypercube sampling to evaluate the pedestrian safety of 32 theoretical bumper designs. There are a total of 9 continuous variables in each design, and the study's conclusion gives values for four pedestrian protection impact criteria as functions of these variables [4]. It should be noted that while regulation only includes three impact criteria, this study separates tibial acceleration into two separate equations, as there are often two acceleration peaks in a typical pedestrian impact. In order to find the outboard stiffness of the middle energy absorber in terms of our design variables, we used it's depth (Dm), height (Hm), and compressive modulus (Em) to model it as a linear spring. This calculation is shown below in Equation 2.

$$S_m = H_m * E_m * 2 / D_m \quad \text{Eq. 2}$$

We can now relate our design variables to the approximate pedestrian safety functions given in the study. This is shown in Equations 3-6 below. These complicated functions are the result of a major corporation's use of heavy computational resources, and approximate the results of each of the 32 FEA simulations they ran.

$$\begin{aligned} \text{Accel1} = & -282.2 + 1.24*Yu + 0.185*Ym - 0.128*Yl - 0.93*Zu - 2.8*Zl + 1922.6*Su - 3.5*Dm... \\ & -252*Sl - 0.0019*Yu*Ym - 0.001*Yu*Yl - 2.37*Yu*Su - 0.225*Yu*Sm + 0.0019*Yu*Dm... \\ & + 0.0018*Ym*Yl + 0.0018*Ym*Zu + 0.0037*Ym*Zl + 0.0042*Ym*Dm + 0.725*Ym*Sl... \\ & + 0.0081*Zu*Zl - 14.6*Zl*Su + 0.0124*Zl*Dm - 2.5*Zl*Sl - \text{MaxAccel} \end{aligned} \quad \text{Eq. 3}$$

$$\begin{aligned} \text{Accel2} = & 5263.1 - 4*Yu - 9.15*Ym - 11*Yl + 1.94*Zu + 4.14*Zl - 11359*Su - 308*Sm - 6.3*Dm... \\ & + 1515*Sl + 0.0052*Yu*Ym + 0.0059*Yu*Zu + 0.0191*Yu*Zl + 14.83*Yu*Su... \\ & + 0.5019*Yu*Sm + 0.027*Ym*Yl - 0.0093*Ym*Zu - 0.0082*Ym*Zl + 0.0068*Ym*Dm - 2.51*Ym*Sl... \\ & - 0.0055*Yl*Zu - 0.0387*Yl*bl - 0.012*Zl*Zu - 3.3*Zl*Smp - 9.16*Zl*Sl - \text{MaxAccel} \end{aligned} \quad \text{Eq. 4}$$

$$\begin{aligned} \text{Rotation} = & 79.37 + 0.095*Yu - 0.076*Ym - 0.3*Yl - 0.63*Zu + 0.31*Zl + 721*Su + 27.1*Smp - 1.14*Dm... \\ & - 56.6*Sl - 0.0003*Yu*Ym - 0.00016*Yu*Yl + 0.0004*Yu*Zu - 0.0004*Zu*Zl - 0.87*Yu*Su... \\ & + 0.0008*Yu*Dm + 0.001*Ym*Yl + 0.0007*Ym*Zu + 0.0008*Ym*Dm - 0.0008*Yl*Zl + 0.1261*Yl*Sl... \\ & + 0.0021*Zu*Zl - 4.38*Zl*Su - 0.17*Zl*Sm + 0.0031*Zl*Dm + 0.23*Zl*Sl - \text{MaxRot} \end{aligned} \quad \text{Eq. 5}$$

$$\begin{aligned}
\text{Shear} = & 65.2 - 0.074*Yu - 0.073*Ym - 0.09*Yl + 0.11*Zu - 0.11*Zl + 299*Su - 13.6*Sm - 0.18*Dm... \\
& + 12.7*Sl + 0.00014*Su*Zl - 0.42*Yu*Su + 0.024*Yu*Sm + 0.0002*Yu*Dm - 0.0002*Ym*Zu... \\
& + 0.0003*Ym*Zl - 0.0245*Ym*Zl - 0.0002*Yl*Zl + 0.0155*Yl*Sl... \\
& - 0.0003*Zu*Zl - 0.3046*Zl*Su + 0.0002*Zl*Dm - 0.1738*Zl*Sl - \text{MaxShear}
\end{aligned} \tag{Eq. 6}$$

Pedestrian protection, however, is only a single component of the regulatory performance subsystem. In order to determine the ability of our bumper design to resist damage, many assumptions must be made. In a real-world low speed crash test, the damage to all components is converted into a cost to repair the vehicle. This dollar amount is the value to be minimized for effective performance, but is difficult to model, as all vehicles are constructed differently. Without knowing the specific architecture of the front end, or which components would be damaged in a real-world crash, we estimate the severity of a crash based off of total energy transferred during the crash, and the inboard deflection of the middle energy absorber. This energy absorber is attached at the rear to the vehicle's steel high-speed crash structure, which will not buckle during a 'fender-bender' type crash. It is therefore reasonable to assume that most of the damage will be a result of the deformation of only the leading (middle) energy absorber, which if designed improperly, may do damage to more costly components such as radiators, bumper sensors, headlights. Low speed testing is carried out by ramming the vehicle into a deformable barrier, which is placed at a height near the middle energy absorber, as detailed in Table 2. Assuming that most or all the kinetic energy from the crash is absorbed in the vehicle's middle energy absorber and the deformable barrier, and that these exert equal force on each other, the bumper deflection can be found from a rudimentary form of the work-energy theorem. For the purposes of this calculation, we model the energy absorbers as linear springs, and assume that deflection is a linear function of force. While real-world energy absorbers are complexly designed and molded to deform in specific patterns, considering the many different non-linear deformation modes of these designs would require heavy engineering simulation. We therefore assume that the cost to repair a vehicle can be estimated by calculating the total bumper intrusion per equation 7, and multiplying it by some constant having the units of \$ USD/mm of intrusion.

$$I_M = \frac{V_{test}}{S_M} \sqrt{\frac{M_{vehicle}}{\frac{1}{S_M} + \frac{1}{S_B}}} \tag{Eq. 7}$$

Equation 7: Total bumper intrusion

Where the test speed V_{test} is set to 1.1 m/s (0.7 mph) in the simulation, and the mass $M_{vehicle}=1500\text{kg}$, the approximate weight of a Toyota Camry. This test speed is representative of standard regulatory bumper testing, and S_B , the stiffness of the PP test barrier, is assigned the a value using the compressive modulus of PP and a similar method to Equation 2 [5].

Equations 3-7 comprise all the relevant measurements for a bumper's regulatory performance, and can be combined into a single equation, shown below.

$$Performance = k3 * Accel1 + k4 * Accel2 + k5 * KneeRot + k6 * KneeSh + k7 * Intrusion \quad \text{Eq. 8}$$

These evaluated regulatory constraints (1st leg acceleration peak, 2nd leg acceleration peak, knee bending, knee shear, vehicle-vehicle crash intrusion) have maximal values which are not to be exceeded for a 'street-legal' vehicle.

Now that the performance evaluations are set up, one can model how cost will be calculated. After making several assumptions about the design norms and manufacturing procedures, a simple model was constructed to approximate cost. Like the equations for regulatory performance, this model is highly idealized, and would have a plethora of additional considerations in real life which are too difficult to model. These include molding technique, established manufacturer infrastructure/expertise, and specific front end architecture. Our research leads to the simplistic cost model shown below in Equation 9, which combines the material and processing prices into a single \$/mm³ occupancy value (which is dependent on which material the middle EA is made of), which is multiplied by the absorber's package space. A width of 2m is assumed for each vehicle.

$$Cost = Hm * Dm * \frac{\$}{mm^3} \quad \text{Eq. 9}$$

Equations 8 and 9 are substituted into Equation 1, and the constraints outlined in the previous section are ensured to be met. With the model constructed, the process of optimization may begin.

Exercising the Model

Initial Attempts and Model Refinement

Our failed attempts at optimization ultimately informed our final model. Before arriving at our well-constrained minimization problem, we explored different initial conditions, solving algorithms, and normalization techniques.

Our first attempts at optimizing the regulatory subsystem indicated that there are many possible optimal designs. The pedestrian protection functions of Equations 3-6 are quite complicated, and made it difficult to use design intuition to evaluate our initial results. The study responsible for creating these functions arrived at their optimal pedestrian safety conditions through constraining pedestrian impact criteria to be below the maximal regulatory values, and seeking to minimize Dm, the inboard package space. Their optimization therefore used these functions in a much simpler capacity, and we had trouble with the high sensitivity caused by combining these equations with low speed crash performance and cost.

During our project, we changed our design variables and parameters as we explored the problem further. During our initial attempts at optimization, we considered outboard stiffness of the middle load path, Sm, as a continuous variable to be optimized, and Hm to be a parameter. This gave us 9 variables

to be optimized for the regulatory subsystem, but the cost would only depend S_m and D_m as variables. In this setup, Equation 2 was a constraint, and S_m and D_m were chosen in optimization such that E_m would match one of the four compressive moduli of the energy absorber materials. Effectively, this method of optimization solved the subsystem in series instead of parallel, and therefore did not find true optimality of the problem. As shown in Table A.1, our results diverged dramatically from minimal perturbations in initial conditions. It was decided to instead treat E_m as a discrete design variable having one value for each of our four material possibilities. The right hand side of Equation 2 was substituted into Equations 3-7, and the corresponding $\frac{\$}{mm^3}$ for each material was substituted into Equation 9. These changes ensured that the subsystems were optimized simultaneously.

This high sensitivity caused us to change our solver and initial condition setup. The default solver for the `fmincon` optimization function is the “interior point” solver. As shown in table A.1, this solver produced highly divergent results, and the arbitrary upper/lower limits we set for our design variables were frequently active constraints. Our initial attempts used 1 as an initial condition for all of our design variables, and the optimization results seemed random. To fix these problems, we decided to make inferences about current designs in order to choose more reasonable initial conditions. Because there are many ways to build the bumper system, we decided to choose 5 initial conditions, and optimize for each: these initial conditions are shown in Table 5. We also replaced the “interior point solver” with the “sqp” algorithm. These two changes gave drastically better results: some starting points did not find optima within our iteration limit, but those that did pointed towards more reasonable solutions.

x(1) Dm	x(2) Zu	x(3) Zl	x(4) Hm	x(5) Ym	x(6) Yu	x(7) Yl	x(8) Em	x(9) Su	x(10) Sl
120	120	60	10	500	740	210	Discrete	0.3	0.25
100	120	50	10	400	700	280	Discrete	0.25	0.2
85	100	20	10	420	680	230	Discrete	0.2	0.15
75	90	30	10	450	640	250	Discrete	0.15	0.2
65	130	10	10	430	660	200	Discrete	0.1	0.15

Table 5: Initial conditions used in the final model. E_m is labeled as “discrete” because it will have one of four values, and the optimization is run for each of these.

Once the subsystems all seemed to be well constrained and interacting well, we faced the problem of weighting and normalization. Our initial objective function (Equation A1) attempted to apply subjective weights to Intrusion, pedestrian safety, and cost. Having three objectives in our minimization problem made it harder to conceptualize, and we decided to combine the intrusion and pedestrian protection functions into a single subsystem, which is shown in Equation 8.

Our early attempts to normalize pedestrian protection values converted each of the results from Equations 3-6 into a value from 0 to 1, where 0 was awarded if the Equations 3-6 yielded below EuroNCAP green rating values, and a 1 signifying that the design barely met lawful maximums for GTR 9. Intrusion was weighted from 0 to 1 as the ratio I_m/D_m : the portion of the total inboard depth of the EA deformed. This normalization and weighting scheme can be seen in Equation A2. Cost was then

normalized in our objective function by dividing by 5, as the performance subsystem was valued from 0 to 1, and so should be cost: 5\$ is very expensive, so this gave somewhat compatible normalization. All in all, our final iteration of the model normalized more organically by recursively comparing the potential of optimal designs. This process is explained in the methodology section along with a discussion of weighting.

Subsystem Optimization and Interaction

Looking at each subsystem independently gives an idea of how they interact with each other. The regulatory subsystem in itself contains five equations for two distinct subparts, and involves all 10 of the design variables. On the other hand, the cost subsystem only depends on 3 design variables, and is handled in one simple equation. It should therefore be noted that the subparts of the regulatory subsystem (pedestrian safety and bumper damage prevention) pose a well-constrained design problem in themselves.

The pedestrian protection portion of the regulatory subsystem represents the most difficult functions to solve. All 10 design variables are involved in Equations 3-6 (because of equation 2, H_m and E_m are included), and the large equations are necessary to represent the interaction of variables for the complex dynamics problem of a vehicle-pedestrian impact. When this subsystem is solved by itself, there are many possible solutions. Having stiff load paths will give different load-path heights and inboard-offsets than soft load paths, and there are a dizzying number of potential solutions to the problem. In themselves, the pedestrian protection functions do not present a solvable optimization problem: additional purpose must be given.

The low-speed crash performance gives that purpose: although this subsystem only includes the variables H_m , E_m , and D_m , these happen to be the most influential variables in the equations for pedestrian safety (coefficients involving S_m , calculated from Equation 2, are larger than average in Equations 3-6, and thus follows the gradient w.r.t. these variables). Pedestrian protection traditionally demands a softer middle bumper system to minimize knee shearing, but damage prevention in vehicle-vehicle crash is best accomplished by using a stiff bumper to minimize intrusion. The regulatory subsystem therefore is optimized differently for every material, because E_m is a chief component in determining the stiffness observed from an outboard location (Equation 2). It is worth noting that if low-speed crash performance was to be optimized individually, the optimal design would be a tall, stiff, bumper, but this conflicts with good pedestrian safety designs, as well as the other subsystem: cost.

The cost of the bumper system's energy absorber is calculated rather simply using the assumptions outlined in the "subsystem background" section. For each material, the cost of the energy absorber can be seen as a linear function of total energy absorber volume (Equation 9). Each material has its own corresponding compressive modulus, E_m , and its own $\frac{\$}{mm^3}$ occupancy value. A minimal cost bumper system would be of the softest material (EPP foam) and would occupy minimal space, but this is unfeasible for both pedestrian safety and low speed damageability.

In summary, viewing each of the subsystems independently does not lead to satisfying optimization problems: their interaction is key to finding a meaningful solution. Table 6 shows the design variables involved in each subsystem (with the regulatory subsystem decomposed into its two parts). Note that Em can be considered as a “material choice” discrete variable, as this same material choice determines the $\frac{\$}{mm^3}$ occupancy value of the absorber. As shown in table 6: Dm, Hm, and Em are involved in every sub-problem.

	Pedestrian	Damageability	Cost
x(1)	Dm	Dm	Dm
x(2)	Zu		
x(3)	Zl		
x(4)	Hm	Hm	Hm
x(5)	Ym		
x(6)	Yu		
x(7)	Yl		
x(8)	Em	Em	Em
x(9)	Su		
x(10)	Sl		

Table 6: Design variables involved in each subsystem

Because three of our ten design variables are so common, the optimization problem as a whole can be seen as the choice of the main bumper component (the middle energy absorber), and the selection of a corresponding front-end shape. The real-world implications of our subsystem interaction is covered after a discussion of our optimization methodology and optimization.

Methodology/Code Structure

The optimization of our system was carried out using Matlab’s built in solver, *fmincon*. However, the default solver package, interior point, was updated to a more robust method: SQP. By implementing the SQP solver, Matlab provided further information about optimization success or failure. This is to say, for each set of initial conditions, given a maximum number of iterations and function evaluations, Matlab could evaluate whether or not a local minimum had been found or whether the solver had failed. This is important because the optimization may not also produce a viable output for the system; if any constraint is violated the solution is rejected and Matlab notes the failure.

In order to further increase the capabilities of the solver, the number of function evaluations and iterations was increased in order to lessen the number of failed solution points. As default values, Matlab allows 3000 function evaluations and 1000 iterations before producing a failed output. The function evaluations and iterations were increased to 1×10^6 and 1×10^4 , respectively.

Scaling each output variable allowed for a weighted, combined objective function. The three output variables are pedestrian protection, crashworthiness (or intrusion), and cost. In order to scale each variable, initial measurements were taken of each output using the objective function as follows:

$$\min f(\mathbf{x}) = \text{Pedestrian Protection} + \text{Crashworthiness} + \text{Cost}$$

This allowed a baseline sample over which the student's t-statistic normalization may be applied; it is given by the following Eq. 10:

$$\frac{X - \bar{X}}{s} \quad \text{Eq. 10}$$

Where X is the individual data point, \bar{X} , is the sample mean and s is the sample standard deviation. In order to produce a well normalized set, this process went through two iterations. The first iteration, as given by the original objective function, had no normalization. Table 7 below summarizes the findings for normalization of each output variable.

Iteration		Crashworthiness	Pedestrian Protection	Cost
1	Mean	0.1634	0.6499	5.3354
	Std Dev	0.1027	0.5871	1.8049
2	Mean	0.1708	0.6500	5.3081
	Std Dev	0.1057	0.6708	1.7814

Table 7: Normalization results from iteration and exercising the model

To create a two dimensional system, pedestrian protection and crashworthiness are summed and given a single weight value. Therefore, cost is assigned the remaining weight. This allows the tradeoffs to be visualized between the aforementioned metrics. The final objective function with variable weighting and normalization then becomes as follows, Eq. 11:

$$\min f(\mathbf{x}) = W \left[\frac{\text{Crashworthiness} - 0.1708}{0.1057} + \frac{\text{Ped. Protect.} - 0.6500}{0.6708} \right] + (1 - W) \left[\frac{\text{Cost} - 5.3081}{1.7814} \right] \quad \text{Eq. 11}$$

Where W is a vector of weight values in the range of 0 to 1.

Once the objective function is established, Matlab runs several loops to analyze the discrete variable for material strength as well as each of the five initial conditions. Although convergence is witnessed between certain initial guesses, it is important to test several as various local minima are observed to exist. The variability of optimal designs is sensible, and was suggested during our research.

Results

Since the model relies on four discrete materials and their respective strengths, the model has been run for several hundred weights in the applicable range for each material. This results in four Pareto curves shown in Figure 4: these are the solutions to the optimization problem.

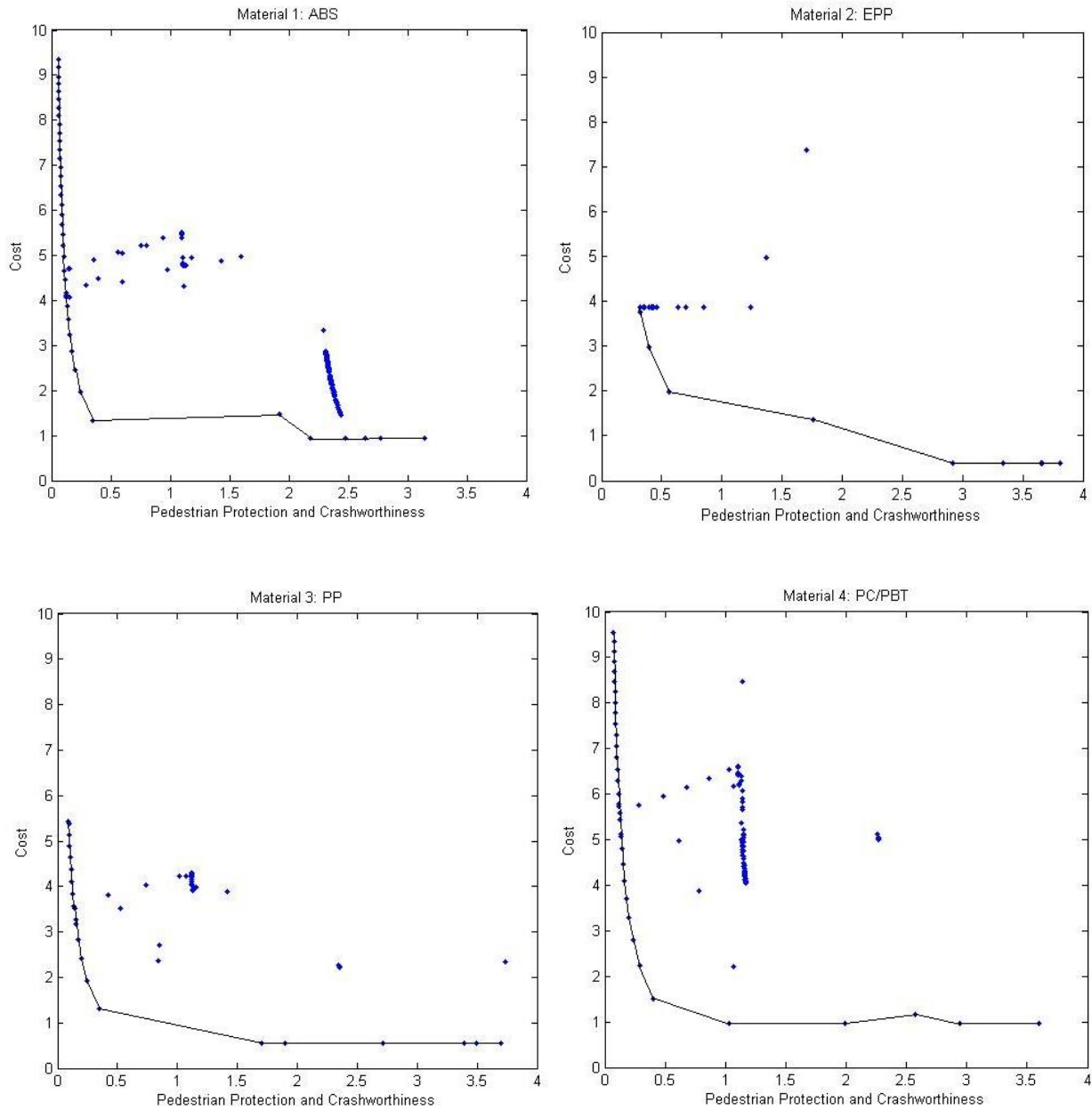


Figure 4: Pareto Curves for each material. Note material choice gives one of the four discrete sets of (E_m and $\frac{\$}{mm^3}$ occupancy). Small values for both subsystems are regarded as optimal.

Given crashworthiness, pedestrian protection, and cost are all output variables to be minimized, there is a clear trade-off between regulatory performance and cost. Note that both subsystems should take on the lowest possible value for optimization: (0,0) in the above sets would be an impossible optima. Each of the four sets shown in Figure 4 are convex, and have interior points representing feasible, sub-optimal designs. Based on all trials over all materials, PP (poly propylene) demonstrates the lowest values for both combined pedestrian protection and crashworthiness and the lowest cost value (0.3447, 1.313) which corresponds to the X^* as follows, with a Weight = 0.0051:

Initial Guess	X1 Dm	X2 Zu	X3 ZI	X4 Hm	X5 Ym	X6 Yu	X7 YI	X8 Em	X9 Su	X10 SI
1	50	106.4296	7.8050	24.1392	387.2918	491.9935	98.9422	1.5	0.5016	3.6342
2	50	120.2252	1.7324	24.1392	475.8608	510.1461	182.0274	1.5	0.1983	2.4505
3	50	101.6926	14.1433	24.1392	390.4693	653.8369	219.1351	1.5	2.2599	9.1157
4	50	91.0864	15.2964	24.1392	396.6979	640.0597	237.9071	1.5	2.0014	9.7778
5	50	131.7610	13.6768	24.1392	385.5335	641.5202	203.7607	1.5	1.9488	8.2320

Table 8: Optimal Solution given Weight = 0.0051

These results are only for PP, so Em can be considered as a parameter here. However, it is interesting to note that each of these five initial guesses converged to the same output values, each of the internal variables did not converge to the same value. Note that Dm, Hm, and Em are the only design variables to converge of these minimizing arguments. This is sensible, as table (7) shows that they are involved in both systems (and all three sub-optimizations). The remaining variables must be such that equations 3-6 give good pedestrian protection values: this is a balance that has many solutions. It is worth noting that this optimal solution has the condition $50mm \leq Dm$ as an active constraint. This minimal value was determined from research, and it can be shown that few of our results have these subjective constraints as active. It is therefore not concerning that Dm attains its minimal value for this “global” solution: a smaller energy absorber is simply not feasible for standard vehicle architectures.

Also notable, this result places high emphasis on the cost of the system. This may not be the true optimal solution to the overall system, as regulatory performance may have much greater worth to a company than that of cost of the system. The results in Table 8 are to be taken with a grain of salt: real-world designs would not use the same weighting in order to find a mathematical ‘global’ minima as seen here: they would balance real-world factors and the many other considerations of vehicle design. Therefore the Pareto curves in Figure 4 should be regarded as our optimal solutions: our results lead to an informed design choice, not a singular solution.

Discussion

As previously noted, the results of this optimization are delivered in the form of four distinct Pareto sets. There are a discreet number of output values, as the solver finds several convergence points. Each Pareto set has over 200 data points, however, this is difficult to visualize because the points often overlap one another. Table 8 is a notable example of output data where design variables are quite different, but the output of pedestrian protection, crashworthiness and cost converge to the same value.

Throughout this optimization project, there have been several setbacks as well as opportunities to learn from mistakes. As previously discussed, the initial solver package, interior point, was not as robust as this optimization required. Matlab did not provide substantial information with the interior point method. Also, using an initial guess far from any optimal point led to very high sensitivity in the

optimization. Since the initial guesses were improved and the solver was changed to SQP, the optimization became far more intuitive and the results were far more consistent and reliable. The SQP solver also allows for repeated analysis – if a certain point is fed back into the solver, the same result will be produced for the set of optimal \mathbf{X} values. This increases the sense of reliability in the process since randomness is eliminated. Before implementing the aforementioned changes to the optimization strategy, a perturbation as small as 0.001 to a single variable caused great variability and sent a red flag that the process was faulted. Reflecting on table A.1 demonstrates the lack of reliability. After implementing the changes, very small perturbations will still converge to the same final, local optimal point.

Overall, we've changed our perception of the optimization problem several times. Re-organizing the subsystems into their current configuration gives us a realistic and visual impression of front-end tradeoffs, as seen in Figure 4.

Real World Application

Due to the nature of this optimization, a single optimization point cannot yet be identified. For such a solution, a singular weight value must be chosen. For example, if a company decides that cost must be minimized and is much more important than the performance metrics, the weight on cost will be higher than that on the performance metrics. This will lead to a smaller cost value but still leaves open the decision of material choice: for a similar cost output, the company may choose the corresponding material with a higher performance metric. Further considerations such as density and overall weight may play crucial deciding factors for the company, but such parameters were not considered in this optimization.

In reality, the subsystems explored here are usually subservient to front-end styling. The headlights, grill, and bumper system are designed extensively to give a pleasing aesthetic: the branding power of the front end is the system's most highly weighted subsystem. For a mathematical optimization process such as this, quantifiable attractive styling has not been implemented. Our simulation is easily adaptable to a real-world design situation. If styling were to be considered first, all state variables except for D_m , H_m , and E_m would be determined. With the shape of the bumper system set by these 7 parameters, the three variables D_m , H_m , and E_m would be optimized in a simulation in order to create a design which excels in regulation and minimizes cost. Perhaps the designing organization excels in manufacturing a single material, or has a limited amount of package space with which to absorb energy: a real world design scenario would see some of our variables turned into parameters.

Overall, the front-end design will be a different problem for each manufacturer and each vehicle, but the optimization model is salient and effective at determining possible designs. The code can be easily adjusted for niche organization use. We've certainly learned about the difficulties of optimization along the way, and can be proud with the results we've produced.

References

1. D. Chon, D. Uikey, R.A. Mohammed, "Energy Absorber Developments and Correlation for Lower Leg Pedestrian Impact", SAE Technical Paper Series, 2007
2. R. Doerr, N. Huda, G. Newlands, T Keer, "Development of Expanded Polypropylene (EPP) Bumper Systems to Meet Emerging Performance and Safety Standards", SAE Technical Paper Series, 2007
3. G. Schroeder, "Manufacturing Cost Analysis of Front-End Package-Space Reduction by Substitution of Advanced TPO", Center for Automotive Research (proprietary), 2013
4. D.K. Nagwanshi, S. Bobba, D. Mana, "Diagnosing Vehicle Aggressiveness for Pedestrian Leg Impact and Development of Efficient Front End Energy Management Systems", SAE International, 2010
5. F. Sofi, S. Kulkarni, M. Haarda, N. Takaaki, Novel Energy Absorber Design "Technique for an Idealized Force-Deformation performance", SAE Technical Paper Series, 2008
6. E. Jaarda, D. Nagwanshi, Prototype "Design and Testing of a Global Energy Absorber Concept for Coupled Pedestrian and Vehicle Protection", SAE Technical Paper Series, 2007

Appendix A: Documentation of failures/learning

	x0									
	x(1)	x(2)	x(3)	x(4)	x(5)	x(6)	x(7)	x(8)	x(9)	x(10)
	Dm	Zu	Zl	Hm	Ym	Yu	Yl	Em	Su	Sl
Trial 1	1	1	1	1	1	1	1	1	1	1
Trial 2	1	1	1	1	1	1	1	1	1.001	1
Trial 3	1	1	1	1	1	1	1	1	1.01	1
Trial 4	1	1	1	1	1	1	1	1	0.999	1
Trial 5	1	1	1	1	1	1	1	1	0.9	1
	x*									
	x(1)	x(2)	x(3)	x(4)	x(5)	x(6)	x(7)	x(8)	x(9)	x(10)
	Dm	Zu	Zl	Hm	Ym	Yu	Yl	Em	Su	Sl
Trial 1	74.417	249.991	6.184	15.000	360.062	555.720	34.658	1.632	0.589	2.018
Trial 2	68.254	247.432	2.420	15.000	424.047	665.663	5.808	3.000	0.802	2.073
Trial 3	54.056	8.809	7.281	15.000	400.060	437.244	93.684	3.000	0.389	3.733
Trial 4	64.625	231.077	1.952	15.000	463.660	488.660	238.384	2.800	0.193	2.516
Trial 5	120.000	221.052	0.000	15.000	172.887	683.504	152.887	0.700	0.486	0.000
	Accel 1	Accel 2	Rotation	Shear	Intrusion %	Pedestrian Safety				
Trial 1	169.983	169.989	18.998	6.000	0.450	3.350E-04				
Trial 2	170.000	170.000	19.000	6.000	0.274	4.364E-07				
Trial 3	170.000	170.000	19.000	6.000	0.282	-6.069E-09				
Trial 4	170.000	169.997	18.999	6.000	0.293	8.273E-05				
Trial 5	102.588	170.000	19.000	6.000	0.720	3.965E-01				

Hm has been exercised as a parameter, Hm = 15, instead of a variable.

Du = DI = 60

Hu = 10

HI = 5

Hmax = 500

Based on the above 5 trials with perturbations ranging from -0.001 to 0.001, it is clear that the optimization is highly sensitive to initial conditions. This optimization was inconclusive because of this dependence on starting condition, although it seemed well bounded. Note, the objective function (Equation A1) had been in no way altered during the five trials. Only the initial condition of Sm (which with Dm determined Em), had been altered.

$$\text{Min } f = \text{Intrusion} * K1 + \text{Pedestrian Protection} * k2 + \text{cost} * k3 \quad \text{Eq. A.1}$$

Our initial three-subsystem objective function used subjective weights and no normalization. It was abandon before the progress report.

$$\text{Performance} = \frac{1}{2} \left(\frac{1}{4} \left(\frac{\text{Accel1}-150}{20} + \frac{\text{Accel2}-150}{20} + \frac{\text{KneeRot}-15}{4} + (\text{KneeSh} - 6) \right) + \frac{Im}{Dm} \right) \quad \text{Eq. A.2}$$

This is the normalization scheme for the performance subsystem that we used in our progress report. Small, insignificant values could become very important and throw off the optimization. Note that the ¼ coefficient in front of the normalized pedestrian safety sum gives a value 0 to 1 for the normalized pedestrian score, and this is again averaged with the normalized intrusion. This gives a total performance score of 0 to 1, which was weighted against cost in our progress report’s objective:

$$\text{Min } f = \text{Performance} * k1 + \frac{\text{cost}}{5} * k2 \quad \text{Eq. A.3}$$

Appendix B: Matlab Code

Optimization model is made of 3 M files: they are divided by blue lines, starting with the main file.

```
clear all

%%%%%%%%%%%%%%%%%%%%%%%%%%%%%%%%%%%%%%%%%%%%%%%%%%%%%%%%%%%%%%%%%%%%%%%%
% Code written by Stephanie Singer and Matthew Schmidt %
% Optimization of Crashworthiness, Pedestrian Protection %
% and Cost for Front End Bumper Fascia. %
% Winter 2015, University of Michigan %
% Mechanical Engineering 555 %
%%%%%%%%%%%%%%%%%%%%%%%%%%%%%%%%%%%%%%%%%%%%%%%%%%%%%%%%%%%%%%%%%%%%%%%%
```

```

global WEIGHT
Hu = 10; %mm
Hl = 5; %mm
Hmax = 500; %
MaxAccel = 170; %m/s^2
MaxRot = 19; %m/s^2
MaxShear = 6; %kN

Vtest = 1.1; %m/s
m_veh = 1500; %kg
Wcrash = 1000; %mm

%ABS EPP PP PC/PBT
materialprice=[9.36*10^-7, 3.86*10^-7,5.4395*10^-7,9.552*10^-07];
materialstrength=[2.5, .4, 1.5, 1.9];
total=zeros(4,6);

i = 1;

valsout = zeros(20,3);
materialindex=3; %choose a material index as specified above
for WEIGHT = [linspace(0, .25,50),linspace(.25,1)]
for j=1:5
xstart =
[120,120,60,10,500,740,210,materialstrength(materialindex),.3,0.25;
100, 120, 50, 10, 400, 700, 280, 1.275, materialstrength(materialindex),
0.2;
85, 100, 20, 10, 420, 680, 230, 1.65, materialstrength(materialindex),
0.15;
75, 90, 30, 10, 450, 640, 250, 2.25, materialstrength(materialindex),
0.2;
65, 130, 10, 10, 430, 660, 200, 2.8, materialstrength(materialindex),
0.15];
x0 = xstart(j,:);
A = [-eye(10);
0 0 0 0 0 0 -1 0 0 0;
0 0 0 1 -1 0 1 0 0 0;
0 0 0 1 1 -1 0 0 0 0;
0 0 0 1 1 0 0 0 0 0;
1 0 0 0 0 0 0 0 0 0;
-1 0 0 0 0 0 0 0 0 0;
0 0 0 1 0 0 0 0 0 0;
0 0 0 -1 0 0 0 0 0 0;
0 0 0 0 -1 0 1 0 0 0;
0 0 0 0 1 -1 0 0 0 0;
0 0 0 0 0 0 0 -1 0 0;
0 0 0 0 0 0 0 1 0 0;
0 1 0 0 0 0 0 0 0 0];
%
B = [zeros(1,10),-Hl,-Hl,-Hu, Hmax, 120,-50, 100, -10, 0, 0, -
.dm+ dm- hm+ hm- ymyl ymyu e- e+ zu
.4,2.5,250];
Aeq = [0 0 0 0 0 0 0 1 0 0]; Beq= [materialstrength(materialindex)];
lb = zeros(1,10); ub = [];
options.Algorithm = 'sqp';

```

```

options.MaxFunEvals = 10e5;
options.MaxIter = 10000;
[sol] = fmincon(@pedobj ,x0, A, B, Aeq, Beq, lb,ub, @func, options);

[x]=sol;
[c] = func(sol);
[A1] = -c(5);
[A2] = -c(6);
[Rot] = -c(7);
[Sh] = -c(8);
Smv = 2*sol(4)*sol(8)/sol(1);

Im = (Vtest/Smv * sqrt(m_veh/((1/Smv)+(1/0.45))))/sol(1);

pedest = (MaxAccel-A1)/MaxAccel + (MaxAccel-A2)/MaxAccel + ...
        (MaxRot - Rot)/MaxRot + (MaxShear-Sh)/MaxShear;

cost=materialprice(materialindex)*sol(1)*sol(4)*2000;

f = WEIGHT*((Im - 0.1708)/0.1057) + ((pedest - 0.65)/.6708) + (1-
WEIGHT)*((cost - 5.3081)/1.7814);

vals(i) = f;

pedval(1,i) = (Im + pedest);
pedval(2,i) = cost;
sols(i,:) = sol;

valsout(i,1) = (Im);
valsout(i,2) = (pedest);
valsout(i,3) = (cost);
valsout(i,4) = ((Im - 0.1708)/0.1057);
valsout(i,5) = ((pedest - 0.65)/.6708);
valsout(i,6) = ((cost - 5.3081)/1.7814);

i = i+1;
end
end %weight end

plot(pedval(1,:),pedval(2,:),'.') %Pareto set
title('Material materialindex');
xlabel('Pedestrian Protection and Crashworthiness');
ylabel('Cost');

valsout

```

```

function [f] = pedobj(x)

MaxAccel = 170;
MaxRot = 19;
MaxShear = 6;
Vtest = 1.1; %m/s
m_veh = 1500; %kg
Wcrash = 1000; %1000mm
global WEIGHT

[c] = func(x);

Accel1 = c(1);
Accel2 = c(2);
Rotation = c(3);
Shear = c(4);

pedest = (MaxAccel-Accel1)/MaxAccel + (MaxAccel-Accel2)/MaxAccel + ...
        (MaxRot - Rotation)/MaxRot + (MaxShear-Shear)/MaxShear;

Smv = 2*x(4)*x(8)/x(1);

Im = Vtest/Smv * sqrt(m_veh/((1/Smv)+(1/0.45)));

if x(8)==2.5
    matindex=1;
elseif x(8)==.4
    matindex=2;
elseif x(8)==1.5
    matindex=3;
else
    matindex=4;
end

materialprice=[0.000000936, 0.000000386,5.4395*10^-7,9.552*10^-07];
cost=materialprice(matindex)*x(1)*x(4)*2000;

f = WEIGHT*((Im - 0.1708)/0.1057) + ((pedest - 0.65)/.6708)) + (1-
WEIGHT)*((cost - 5.3081)/1.7814);

end

```

```

function [c, ceq] = func(x)

%%%%%%%%%%%%%%%%%%%%%%%%%%%%%%%%%%%%%%%%%%%%%%%%%%%%%%%%%%%%%%%%%%%%%%%%
% The following equations come from the SAE International paper: %
%"Diagnosing Vehicle Aggressiveness for Pedestrian Leg Impact and %
% Development of Efficient Front End Energy Management Systems" %
% Authors: Nagwanshi, Bobba and Mana, GE India %

```

%%%

```
MaxAccel = 170;  
MaxRot = 19;  
MaxShear = 6;
```

```
%X =[ Dm Zu Zl Hm Ym Yu Yl Em Su Sl]
```

```
Smp = x(4)*x(8)*2/x(1);
```

```
Accel1 = -282.2 + 1.24*x(6) + 0.185*x(5) - 0.128*x(7) -0.93*x(2) - 2.8*x(3) +  
1922.6*x(9) -3.5*x(1) ...  
-252*x(10)-0.0019*x(6)*x(5) - 0.001*x(6)*x(7) - 2.37*x(6)*x(9) -  
0.225*x(6)*Smp + 0.0019*x(6)*x(1) ...  
+ 0.0018*x(5)*x(7) + 0.0018*x(5)*x(2) + 0.0037*x(5)*x(3) + 0.0042*x(5)*x(1)  
+ 0.725*x(5)*x(10) ...  
+0.0081*x(2)*x(3) - 14.6*x(3)*x(9) + 0.0124*x(3)*x(1) - 2.5*x(3)*x(10) -  
MaxAccel;
```

```
Accel1p = -282.2 + 1.24*x(6) + 0.185*x(5) - 0.128*x(7) -0.93*x(2) - 2.8*x(3)  
+ 1922.6*x(9) -3.5*x(1) ...  
-252*x(10)-0.0019*x(6)*x(5) - 0.001*x(6)*x(7) - 2.37*x(6)*x(9) -  
0.225*x(6)*Smp + 0.0019*x(6)*x(1) ...  
+ 0.0018*x(5)*x(7) + 0.0018*x(5)*x(2) + 0.0037*x(5)*x(3) + 0.0042*x(5)*x(1)  
+ 0.725*x(5)*x(10) ...  
+0.0081*x(2)*x(3) - 14.6*x(3)*x(9) + 0.0124*x(3)*x(1) - 2.5*x(3)*x(10);
```

```
Accel2 = 5263.1 - 4*x(6) - 9.15*x(5) - 11*x(7) +1.94*x(2) + 4.14*x(3) -  
11359*x(9) - 308*Smp - 6.3*x(1) ...  
+1515*x(10) + 0.0052*x(6)*x(5) + 0.0059*x(6)*x(2) + 0.0191*x(6)*x(3) +  
14.83*x(6)*x(9) ...  
+0.5019*x(6)*Smp + 0.027*x(5)*x(7) - 0.0093*x(5)*x(2) - 0.0082*x(5)*x(3)  
+ 0.0068*x(5)*x(1) - 2.51*x(5)*x(10) ...  
-0.0055*x(7)*x(2) - 0.0387*x(7)*x(3) - 0.012*x(3)*x(2) - 3.3*x(3)*Smp -  
9.16*x(3)*x(10) - MaxAccel;
```

```
Accel2p = Accel2 + MaxAccel;
```

```
Rotation = 79.37 + 0.095*x(6) - 0.076*x(5) - 0.3*x(7) - 0.63*x(2) + 0.31*x(3)  
+ 721*x(9) + 27.1*Smp - 1.14*x(1) ...  
-56.6*x(10) - 0.0003*x(6)*x(5) - 0.00016*x(6)*x(7) +0.0004*x(6)*x(2) -  
0.0004*x(2)*x(3) - 0.87*x(6)*x(9) ...  
+0.0008*x(6)*x(1) + 0.001*x(5)*x(7) + 0.0007*x(5)*x(2) + 0.0008*x(5)*x(1)  
- 0.0008*x(7)*x(3) + 0.1261*x(7)*x(10) ...  
+0.0021*x(2)*x(3) - 4.38*x(3)*x(9) - 0.17*x(3)*Smp + 0.0031*x(3)*x(1) +  
0.23*x(3)*x(10) - MaxRot;
```

```
Rotp = Rotation + MaxRot;
```

```
Shear = 65.2 - 0.074*x(6) - 0.073*x(5) -0.09*x(7) + 0.11*x(2) - 0.11*x(3) +  
299*x(9) - 13.6*Smp - 0.18*x(1) ...  
+12.7*x(10) + 0.00014*x(9)*x(3) - 0.42*x(6)*x(9) + 0.024*x(6)*Smp +  
0.0002*x(6)*x(1) - 0.0002*x(5)*x(2) ...  
+0.0003*x(5)*x(3) -0.0245*x(5)*x(3) - 0.0002*x(7)*x(3) +  
0.0155*x(7)*x(10) ...  
-0.0003*x(2)*x(3) - 0.3046*x(3)*x(9) + 0.0002*x(3)*x(1) -  
0.1738*x(3)*x(10) - MaxShear;
```

```
ShearP = Shear + MaxShear;
```

```
c = [Accel1; Accel2; Rotation; Shear; -Accel1p; -Accel2p; -Rotp; -ShearP];  
ceq = [];
```

```
end
```